ELSEVIER

Thermochimica Acta 292 (1997) 159–168

thermochimica acta

An analysis method for nucleation and growth controlled reactions at constant heating rate

M.J. Starink*, A.-M. Zahra

Centre de Thermodynamique et de Microcalorimétrie du CNRS, 13331 Marseille Cedex 3, France

Received 16 September 1996; accepted 21 November 1996

Abstract

A quantitative model is derived for the progress of a nucleation and growth controlled reaction during heating at a constant rate. It incorporates nucleation, growth, and impingement, takes account of temperature dependent solubility, and distinguishes between diffusion controlled growth and linear growth. Parameters of the model for a single process reaction are: s, which is akin to the Avrami parameter for isothermal analysis, E_{eff} the effective activation energy, η_i the impingement parameter, and a pre-exponential constant. The model is applied to the DSC data on precipitation in Al–Si alloys. An excellent agreement between data and model is obtained. The parameter s is interpreted in terms of the processes taking place, namely growth of small nuclei, growth of coarse particles or nucleation and growth. © 1997 Elsevier Science B.V.

Keywords: Al–Si alloys; Differential scanning calorimetry (DSC); Johnson–Mehl–Avrami–Kolmogorov (JMAK) model; Non-isothermal analysis; Nucleation and growth

1. Introduction

Isothermal transformation data for reactions which proceed via nucleation and growth are often analysed using the so-called Johnson–Mehl–Avrami–Kolmogorov (JMAK) [1–5] equation. In generalised form, this equation gives the fraction transformed, α, as a function of time, t:

$$\alpha = 1 - \exp[-(k(T)t)^n] \quad (1)$$

where n is a constant, often referred to as the Avrami exponent and $k(T)$ the temperature-dependent factor. The above expression can often fit isothermal transformation data at least for small α, and conclusions concerning the reaction mechanism can be drawn from the calculated values of n [6,7].

Whereas isothermal experiments are generally time consuming, experiments performed at constant heating rate are a far more rapid way of studying a transformation. Hence, experimental methods like differential scanning calorimetry (DSC) or thermogravimetry (TG) have gained popularity. For an analysis of these experiments, it would be advantageous to obtain an equation based on the same principles as the JMAK equation. In any attempt to derive such an equation, several problems need to be addressed. Firstly, one has to consider the status of the JMAK equation for isothermal studies and the assumptions made in deriving it. In considering this point, it is important to note that often the JMAK equation fits isothermal transformation data only over a very small

*Corresponding author. Present address: IPTME, University of Technology, Loughborough LE 11 3TU, UK

PII S0040-6031(96)03135-8

range of α and that better fits can be obtained using the so-called Austin–Rickett (AR) kinetic equation [8]:

$$\alpha = 1 - [(k(T)t)^n + 1]^{-1} \quad (2)$$

Secondly, one needs to consider whether assumptions made for the isothermal case are still valid for the non-isothermal case. Here, it is important to note that the case of constant nucleation rate, as is often assumed for isothermal experiments, will generally not occur for experiments performed at constant heating rate. Further, one needs to find a correct way to obtain the temperature integral of the JMAK equation.

In this work, a new method for analysing nucleation and growth transformations at constant heating rate is introduced. This method starts from the microscopic level, namely the growth law (dimensionality of the growth) of a single precipitate. It takes account of the heating rate, activation energies for nucleation and growth, the Avrami exponent, impingement and the temperature dependence of the equilibrium state. The model is applied to precipitation in Al–Si alloys.

2. Experimental

2.1. Alloys

DSC experiments were performed on high purity Al–1at%Si and Al–6at%Si alloys which were produced by conventional casting. The Al–1at%Si alloy was homogenised at 550 ± 10°C for 20 h. Chemical analysis showed the following composition: 1.0at%Si, 0.002at%Cu, 0.003at%Fe, balance Al. In every case, DSC samples were machined prior to solution heat treatments. Some Al–1at% Si samples were solution treated for 2 h at 575°C and then cooled (cooling rate ca. −22°C/min) inside the DSC apparatus. Other samples were solution treated for 2 h at 550°C and, subsequently, quenched in iced water (IWQ=ice-water quench). The Al–6at%Si alloy showed a composition of 5.8 ± 0.1at%Si. It was solution treated for 2 h at 550°C and either cooled inside the DSC (at ca. −200°C/min) or quenched in iced water.

2.2. Differential scanning calorimetry

For the DSC experiments, two types of DSC apparatus were employed: a Perkin–Elmer 1020 series DSC7 and a Dupont type 910. For the experiments on Al–1at%Si samples, cooled at −22°C/min, the Dupont 910 apparatus was used and the experimental details are presented in [9,10]. For all other DSC experiments, the Perkin–Elmer DSC7 was used with samples of 6 mm diameter and 1 mm height (average mass ~70 mg). (For a description of the Perkin–Elmer DSC system and its performance see [11].) For all the experiments, reference samples with dimensions close to those of the alloy samples were used (i.e. heat capacity differences are small). The heat flow is calibrated by measuring the heat of fusion of In. The temperature is calibrated by taking the deviation, ΔT, from the reference temperature equal to the following expression:

$$\Delta T = \Delta T_0 + pT + \tau\beta \quad (3)$$

(T in °C), where β is the heating rate, p a (small) constant, τ the parameter representing the time constant of the DSC apparatus in combination with the sample used [11], and ΔT_0 represents ΔT extrapolated to $\beta = 0$. ΔT_0 and p are determined by measuring the onset of melting of pure In and Zn at various heating rates and subsequently extrapolating to zero heating rate, while τ is determined from the variation of the onset of eutectic melting with heating rate in an Al–16at% Mg alloy sample[1] of size similar to the Al–Si samples. The value of τ (9.94 s) compares well with values determined earlier for samples of similar mass [11].

Experiments using pure aluminium as sample and reference material showed that the baseline of the Perkin–Elmer DSC7 varied day-to-day in an irregular manner. The heat flow rate of this type of baseline can be well described by:

$$\frac{dq}{dt} \equiv \dot{q} = a + bT + cT^3 \quad (4)$$

where T is measured in °C. As the heat capacity of aluminium and silicon in the temperature range con-

[1]This Al–16%Mg alloy is close to ideal for the determination of τ of a DSC apparatus in conjunction with Al-based alloy samples as: (i) the eutectic reaction which is due to melting of β phase particles, occurs at a well-defined temperature of 450°C; (ii) eutectic melting only occurs at grain boundaries, i.e. heat flow in the sample occurs through a solid Al-based alloy; and (iii) the heat effect due to eutectic melting is of the same order as the precipitation reactions in Al-based alloys. DSC and TEM work on Al–Mg alloys will be presented elsewhere [12].

sidered may be described reasonably well with Eq. (4), Kopp and Neumann's additivity rule indicates that the heat capacity of Al–Si can also be approximated reasonably well with the above equation. As the difference in heat capacity between sample and reference is small, it is justified to use Eq. (4) to obtain baselines which represent heat flow due to both heat capacity differences and imperfections of the DSC apparatus. To obtain the heat flow due to reactions, $\dot{q}_R$, measured DSC curves were corrected by obtaining a, b and c corresponding to a best fit using the following criteria:

(i) for all alloys: before the precipitation effect $\dot{q}_R = 0$;
(ii) if the dissolution effect in the alloy is completed before the end of the DSC run: $\dot{q}_R = 0$ after the completion of the dissolution effect; and
(iii) if the dissolution effect in the alloy is not completed before the end of the DSC run: the total heat effect of precipitation equals the total heat effect of re-dissolution of the precipitated phases up to the solution treatment temperature (550°C for the Al–6at% Si alloy).

As a maximum of 1.6 at% of Si can be dissolved in the Al-rich phase, criterion (ii) is used for the Al–1at%Si alloy, whereas (iii) is used for the Al–6at%Si samples. Generally all criteria can be met with an accuracy better than 1%. (Here, the fraction of deviation from $\dot{q}_R = 0$ is given with respect to the maximum observed heat flow.)

3. Analysis method for precipitation reactions at constant heating rate

Recently, it was shown [8] by one of the present authors that the kinetics of transformation for precipitation reactions could mostly be described well by the Austin–Rickett equation (Eq. (2)). On the other hand, it was also found that the JMAK equation (Eq. (1)) fitted well to data of pearlitic transformations. Hence, to study transformation processes in general, it is desirable to use one single equation which incorporates both the AR and the JMAK equations. In the following, we will develop such a general equation and obtain solutions for non-isothermal experiments at a linear heating rate. In Section 4 we will apply it to study the DSC data.

3.1. Nucleation and growth in the extended volume

As in the works of Johnson and Mehl [1] and Avrami [2–4], the transformation is described using the so-called 'extended volume' concept. In the 'extended volume' the individual nuclei grow without any limitation of space. In applying this concept, first the volume, V_p, of the transformed region at time t which nucleated at an earlier time z will be calculated. Whilst in many reactions (for instance recrystallisation) the boundary between transformed region and untransformed region is sharp and the definition of V_p is clear, for diffusion controlled precipitation reactions, the definition of V_p is not immediately obvious, as in the diffusion zone there is a gradual change from transformed, fully depleted to an untransformed matrix which is undepleted. Here, we will define the transformed volume to be that volume of an imaginary fully depleted area around a precipitate (with the rest of the matrix undepleted), needed to give a precipitate size equal to the real case with a diffusion zone.

In general, the following holds:

$$V_p = A_1[G(t-z)]^m \tag{5}$$

where G is the (average) growth rate, A_1 a constant, related to the initial supersaturation, the dimensionality of the growth and the mode of transformation, and m a constant, related to the dimensionality of the growth and the mode of transformation (diffusion controlled growth or linear growth). An overview of the values of m that occur for different types of reactions has been given by Christian [6]. For the case of diffusion controlled growth for several geometries, A_1 can be obtained from the work of Coates [13]. For the purpose of the present paper, mainly diffusion controlled growth in three dimensions is important. For this case, $m = 1\frac{1}{2}$.

Next the contribution of nucleation is considered. The contribution of the particles which nucleated during the time interval $(z, z + dz)$ to the amount of volume transformed in the 'extended volume' at time t, $V_{ext}(t)$ is obtained by using Eq. (5):

$$dV_{ext} = A_1 I(z) V_0 [G(t-z)]^m dz$$

where $I(z)$ is the nucleation rate per unit volume. Integrating and introducing $\alpha_{ext} = V_{ext}/V_0$, where V_0 is the volume of the sample, yields:

$$\alpha_{ext} = \int_0^t A_1 I(z)[G(t-z)]^m dz \quad (7)$$

Generally, the growth rate is ruled by diffusion and hence, can be approximately described by an Arrhenius-type temperature dependence:

$$G(T) = G_0 \exp\left(\frac{-E_G}{k_B T}\right) \quad (8)$$

Woldt [14], Krüger [15] and de Bruijn et al. [16] assumed that the nucleation rate can also be approximated by an Arrhenius-type temperature dependence, that is:

$$I(T) = I_0 \exp\left(\frac{-E_N}{k_B T}\right) \quad (9)$$

where k_B is the Boltzmann constant, and E_G and E_N are the activation energies for growth and nucleation, respectively. The latter equation (Eq. (9)) implies that nucleation depends only on the mobility of atoms. In particular, when the driving force for the formation of nuclei (i.e. change in Gibbs free energy due to the transformation of a region) is small, Eq. (9) may not hold any more. However, here we consider nucleation during heating (i.e. the experiment starts at low temperature), and thus the driving force for formation of nuclei will generally be large and the current approximation will be valid. Eq. (9) leads to a relatively simple expression for α_{ext}, as from Eqs. (7)–(9) it follows (see [14,15]):

$$\alpha_{ext} \cong \left(\frac{\beta k_B}{E_G} k_c \exp\left[\frac{-E_{eff}}{k_B T}\right]\left(\frac{T}{\beta}\right)^2\right)^s \quad (10)$$

where,

$$E_{eff} = \frac{mE_G + E_N}{m+1} \quad (11)$$

$$s = m + 1 \quad (12)$$

and k_c is a constant. It should be noted that Eq. (10) is an approximation which is only accurate if $E_N \approx E_G$ (see [14]).

To illustrate the use of Eq. (10), we consider a reaction with $m = 3$ (e.g. valid for recrystallisation) and nucleation rate according to Eq. (9). Then Eq. (10) shows that, for an experiment at constant heating rate, α_{ext} increases in proportion to $t^{2(m+1)} = t^8$. For comparison, in an isothermal experiment, α_{ext} increases in proportion to $t^{m+1} = t^4$ (see also [14]).

It is also seen that when nuclei are present before the start of the transformation and no further nucleation occurs, Eq. (10) is valid to a good approximation [14,15]. In this case, $s = m$ and $E_{eff} = E_G$. Thus, providing Eqs. (8) and (9) are valid, s equals the so-called Avrami exponent n, as it appears in Eq. (1).

3.2. Impingement

To obtain a general kinetic equation, the effect of impingement should be included. Here, we will simply state that both the AR (Eq. (2)) and the JMAK equations (Eq. (1)) can be derived from:

$$\frac{d\alpha}{d\alpha_{ext}} = (1-\alpha)^{\lambda_i} \quad (13)$$

where λ_i will be termed the impingement factor (see also [17]). (Note that for the case of no impingement, i.e. $\alpha_{ext} = \alpha$, $\lambda_i = 0$.} The JMAK equation is obtained for λ_i=1, while Eq. (2) is obtained for λ_i=2. The general solution of Eq. (13) for $\lambda_i = 1$ is,

$$\alpha = 1 - \left(\frac{\alpha_{ext}}{\eta_i} + 1\right)^{-\eta_i} \quad (14)$$

where $\eta_i = 1/(\lambda_i - 1)$. For λ_i=1, the solution is:

$$\alpha = 1 - \exp(-\alpha_{ext}) \quad (15)$$

Alternatively, an expression equivalent to Eq. (15) is obtained from Eq. (14) for the limit of $\eta_i \to \infty$ and, hence, Eq. (14) incorporates Eq. (15). Thus, by fitting the combination of Eqs. (10) and (14) to experimental transformation data, the parameters obtained, s and η_i, will give information about the mechanism of the reaction. (Further, the case of no impingement, $\lambda_i = 0$, can also be described by Eq. (14).)

In some precipitation reactions, several processes with different s can occur. As examples, consider (i) the simultaneous occurrence of grain boundary precipitation and precipitation in grains, or (ii) the simultaneous growth of pre-existing nuclei and the

nucleation and subsequent growth of new nuclei. When impingement of precipitates formed by dissimilar processes is negligible as compared to impingement between precipitates formed by the same process, the processes essentially occur in independent volumes of the alloy, and the sum of two processes is obtained simply from a weighted average:

$$\xi = f\xi_1 + (1-f)\xi_2 \tag{16}$$

where f is the volume fraction of the alloy in which process 1 occurs, and $(1-f)$ the volume fraction of the alloy in which process 2 occurs, while ξ is the amount of atoms incorporated in the growing nuclei divided by the maximum amount of atoms that can be incorporated according to the equilibrium phase diagram.

3.3. Temperature dependence of the equilibrium state

So far, the foregoing treatment has not taken into account the variation of the equilibrium state with temperature. To account for this the following treatment is proposed: Consider the concentration in the matrix, adjacent to a precipitate, to be equal to the equilibrium or metastable equilibrium concentration, $c_{eq}(T)$ (the so-called 'localised equilibrium' assumption). Further, assume that the variation of $c_{eq}(T)$, as a result of the increase in temperature is relatively slow as compared to the variation in the local concentrations of the alloying atoms, due to the diffusion of atoms. This means that the local concentrations of alloying atoms in the matrix, $c(x, y, z, t, c_{eq}(T))$, can be obtained in good approximation from the concentrations, as in the hypothetical case, where c_{eq} is constant:

$$c_0 - c(x,y,z,t,c_{eq}(T)) = [c_0 - c(x,y,z,t,c_{eq}=0)]\frac{c_0 - c_{eq}(T)}{c_0} \tag{17}$$

The number of atoms transformed in the course of the reaction is proportional to the volume average of the left-hand side of Eq. (17). The volume average of the term $[c_0 - c(x,y,z,c_{eq}=0)]$ is proportional to α for the case, where c_{eq} is constant. This latter case led to Eqs. (10) and (14). Hence, it follows:

$$\frac{d\xi}{dt} = A_2\frac{d}{dt}\left[\alpha\frac{c_0 - c_{eq}(T)}{c_0}\right] \tag{18}$$

where A_2 is a constant. Here again, it is assumed that the variation of $c_{eq}(T)$ as a result of the increase in temperature is relatively slow as compared to that due to diffusion of atoms.

Because $d\xi/dt$ is proportional to the heat effect caused by a reaction, the combination of Eqs. (10), (14) and (18) can be used to fit heat effects due to precipitation reactions. The fit is based on the solubility $c_{eq}(T)$ and the reaction parameters η_i, s and E_{eff}. The latter two are related to m and the activation energies for growth and for nucleation, respectively.

3.4. Determination of activation energies

From Eq. (10), it follows that for temperature, T_f, at constant α_{ext}:

$$\ln\frac{\beta}{T_f^2} = -\frac{E_{eff}}{k_B T_f} + C_1 \tag{19}$$

C_1 is a constant which depends on the reaction stage. This equation is similar to the one used in the so-called Kissinger method, but the latter is usually obtained via different set of assumptions. We will review the derivation of the Kissinger method below:

In many publications, the transformation rate during a reaction is assumed to be the product of two functions, one depending solely on temperature, T, and the other depending solely on the fraction transformed:

$$\frac{d\alpha}{dt} = k(T)f(\alpha) \tag{20}$$

Usually, an Arrhenius expression is assumed to be valid for $k(T)$, i.e.:

$$k(T) = k_0\exp[-E_A/k_B T] \tag{21}$$

where k_0 is a constant, E_A the apparent activation energy of the process, which is assumed to be constant. Methods for determining E_A can be derived as follows: Eq. (20) is integrated by separation of variables (using $dT = \beta dt$):

$$\int_0^\alpha \frac{d\alpha}{f(\alpha)} = \frac{k_0}{\beta}\int_0^{T_f}\exp\left(-\frac{E_A}{k_B T}\right)dT \equiv \frac{k_0 E_A}{\beta k_B}\int_{y_f}^{\infty}\frac{\exp(-y)}{y^2}dy = \frac{k_0 E_A}{\beta k_B}p(y_f) \tag{22}$$

where $y = E_A/k_BT$, $y_f = E_A/k_BT_f$, T_f is the temperature at a fixed state of transformation. Various ways of approximating $p(y)$ have been applied in the literature (see [18–20]). Integrating in parts and truncating the series by assuming $y_f \gg 1$ results in the following approximation for p (see [18,21]):

$$p(y) \cong \frac{\exp(-y)}{y^2} \tag{23}$$

The assumption $y_f \gg 1$ is reasonable, since for the vast majority of solid-state reactions (and many other reactions) $15 < y_f < 60$. At constant fraction transformed this leads to:

$$\ln\frac{\beta}{T_f^2} = -\frac{E_A}{k_BT_f} + C_2 \tag{24}$$

C_2 is a constant which depends on the reaction stage as well as on the kinetic model. According to Eq. (24), plots of $\ln(T_f^2/\beta)$ vs. $1/T_f$ should result in straight lines, with slopes E_A/k_B. This method for the calculation of E_A is usually referred to as the (generalised) Kissinger method.

Comparison of Eqs. (19) and (24) shows that the two approaches lead to similar equations for deriving activation energies. There are, however, important differences, i.e. $E_A = E_{eff}$ is only valid under the proviso that a constant α_{ext} implies a constant α. According to the theory in Sections 3.1–3.3, this is the case (i) if the impingement parameter is independent of heating rate, and (ii) in the limit $\alpha \to 0$.

In a previous paper [21], it was shown that the Kissinger analysis is more accurate than the so-called Ozawa method, which is derived on the basis of a different approximation for $p(y)$. It was also found that the following expression is even more accurate than the Kissinger method:

$$\ln\frac{\beta}{T_f^{1.8}} = -A\frac{E_A}{k_BT_f} + C_3 \tag{25}$$

with

$$A = 1.0070 - 1.2 \times 10^{-5}E_A \quad (E_A \text{ in kJ/mol}) \tag{26}$$

C_3 is a constant which depends on the reaction stage and on the kinetic model. Hence, in order to obtain the activation energy with this new method, the slope of a plot of $\ln(T_f^{1.8}/\beta)$ vs. $1/k_BT_f$ should be calculated, while A can be evaluated using this slope as a first approximation for E_A.

4. Results and discussion

In this section, we will apply the expressions derived in the previous section to analyse the precipitation effect in Al–Si alloys. These alloys are especially suited for evaluation of the validity of the presented theory because, in these alloys, Si always precipitates in the form of the equilibrium diamond cubic Si phase. The solubility of Al in this phase is negligible. Further, the equilibrium solubility of Si in the Al-rich phase is well established. It can be represented by [22]:

$$c_{Si}(T) = c_\infty \exp\left(-\frac{\Delta H_{Si}}{k_BT}\right) \tag{27}$$

where $\Delta H_{Si} = 54$ kJ/mol ($= 0.52$ eV) and $c_\infty = 19$.

Before presenting the experiments and the fits based on the proposed theory, a few remarks concerning the manner of fitting and the type of processes expected to occur are in order. These are as follows:

(i) Some rearrangement of Eq. (10) shows that the dominating temperature dependent term of this equation is $\exp(-sE_{eff}/k_BT)$. This shows that from one experiment, only the product $s \times E_{eff}$ can generally be derived accurately (see also [23,24]). Hence, it is necessary to obtain an activation energy using experiments at different heating rates (or isothermal experiments at different temperatures). Throughout this work, we will use the value $E_{eff} = 101$kJ/mol (0.97 eV) as obtained previously from a DSC study of precipitation in Al–1at% Si [9].

(ii) In isothermal analysis of a process which corresponds to JMAK kinetics, the Avrami parameter, n, for the start of the process can generally be obtained from the slope of the plot of $\ln[-\ln(1-\alpha)]$ vs. $\ln(t)$. Similar procedures can be derived for a non-isothermal JMAK process at constant heating rate (see, e.g. [14,24]). For instance, Criado [24] showed that, in good approximation, a plot of $\ln[-\ln(1-\alpha)]$ vs. $1/T$ gives a straight line, the slope of which yields $n \times E_{eff}$. This method is, however, only valid if the equilibrium state is constant. The latter provision is not valid in our alloys and, hence, this method cannot be applied in the

present work. However, plots of the measured and calculated $\ln \dot{q}_R$ vs. the temperature are observed to be approximately linear over the first part of the reaction, with the slope of the calculated $\ln \dot{q}_R$ vs. the temperature varying strongly with s. Hence, by comparing plots of measured and calculated $\ln \dot{q}_R$ vs. the temperature, the appropriate value of s for the process which dominates the initial stage of the reaction is readily identified. If more than one process occurs, the process which dominates the initial stage of the reaction is always the process with the lowest s value.

(iii) It is generally thought that the precipitation in Al–Si occurs via the formation of Si clusters [25–27] which can form at low temperatures before any detectable formation of the equilibrium Si phase. Hence, depending on heat treatment, nuclei may be present in these alloys.

In Fig. 1, a DSC experiment performed on an Al–1at%Si alloy which was cooled at −22°C/min after solution treatment, is presented. Because this cooling rate is quite slow and barely sufficient to avoid precipitation, a high density of nuclei can be expected to be formed during the cooling. In Fig. 1, the fit based on the theory presented in Section 3, with one single process operating, is also given. For the fit, $d\xi/dt$ was calculated according to Eqs. (10),(14),(16) and (18) and normalised to obtain a maximum exothermic heat flow identical to that in the experiments. Fig. 1 shows a near perfect match between theory and experiment. The value of s obtained (1.65) is close to the value expected for growth of pre-existing nuclei ($1\frac{1}{2}$). This indicates that precipitation occurs nearly exclusively by growth of pre-existing nuclei. Hence, the s value resulting from our analysis method conforms well with expectations outlined above.

Fig. 2 presents a DSC experiment performed on an Al–1at% Si alloy which was aged for nine months at 20°C, subsequent to solution treatment (2 h at 550°C) and IWQ. It may be expected that, due to natural ageing (NA), pre-existing nuclei will be present in this sample but fewer than in the sample cooled at −22°C/min. Hence, the DSC curve was fitted with two processes operating (using Eqs. (10), (14), (16) and (18)) with $s_1 = 1\frac{1}{2}$ for the first process. We will further use η_{i1} obtained from the fit in Fig. 1 (0.63). It was found that the following parameters resulted in the best fit: f = 0.74, and for process 2: $s_2 = 2.66$,

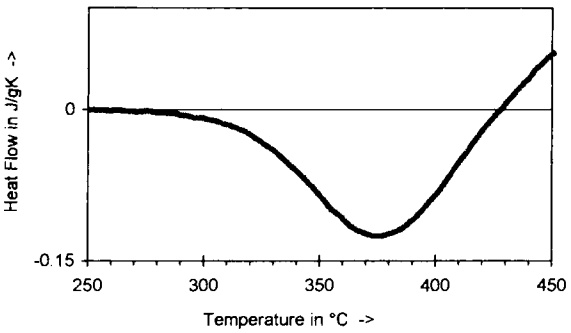

Fig. 1. DSC curve at heating rate 10°C/min of Al–1at% Si which was cooled at −22°C/min after solution treatment (thick, grey line). The fit (thinner, black line) is obtained with the model presented in Section 3 and $s = 1.65$, $\eta_i = 0.63$ and $E_{eff} = 101$kJ/mol.

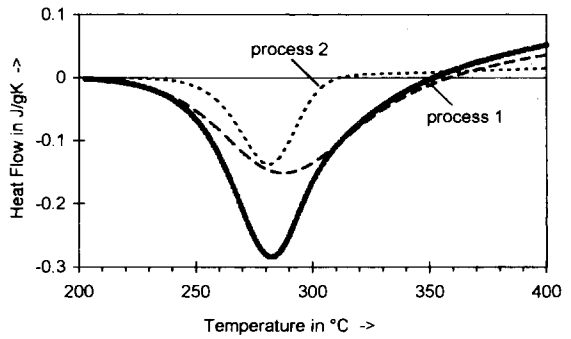

Fig. 2. DSC curve ($\beta = 20$°C/min) of the Al–1at% Si alloy naturally aged for nine months subsequent to solution treatment (thick, grey line). The fit (thinner, black line) is obtained with the model presented in Section 3. Also indicated are the contributions of the two processes.

$\eta_{i2} = 2.2$. The fit presented in Fig. 2 shows a nearly perfect match to the experiment. The obtained value for s_2 is close to the expected one of $2\frac{1}{2}$ for nucleation and subsequent growth of new nuclei. This analysis shows that, for the Al–1at% Si alloy, different cooling rates result in different precipitation processes: after cooling at −22°C/min, precipitation mainly occurs via growth of pre-existing nuclei, while after IWQ and natural ageing, both growth of pre-existing nuclei and new nucleation and growth take place.

It is further noted that, in the IWQ Al–1at%Si alloy, precipitation occurs at lower temperatures than for the Al–1at%Si alloy which was cooled at −22°C/min.

This is thought to be due to a higher vacancy concentration in the IWQ alloy [28].

DSC experiments performed on the same Al–1at% Si alloy, but now naturally aged for only a few minutes, give very similar curves and the fitting parameters are almost the same. Apparently, the overwhelming majority of nuclei that are viable and grow during a DSC experiment at 20°C/min are formed during the quench. This does not mean that during natural ageing no formation of nuclei may occur. It does indicate, however, that if natural ageing causes the creation of a significant number of nuclei, they are apparently small and not viable at the temperatures at which precipitation occurs during the DSC run (~210–350°C). This can be explained in terms of the Gibbs–Thomson effect, that is due to the contribution of interfacial energy to their overall free energy, small nuclei/precipitates experience a metastable solvus which is situated at lower temperatures than the equilibrium one. As a result, if the nuclei formed during ageing are very small, they dissolve before significant precipitation occurs during the DSC run.

In Fig. 3, a DSC experiment performed on an Al–6at%Si alloy which was cooled at −200°C/min after solution treatment at 550°C, is presented. Because the Si content for this alloy is much higher than the solubility at the solution treatment temperature (0.013), coarse undissolved Si particles will be present. It is expected that precipitation will occur initially via growth of these coarse Si particles, and because the size of the Si particles will be much larger than the diffusion distances, this process corresponds to one-dimensional diffusion, that is $m \equiv s = 1/2$ (see [8,13]). Hence, the DSC curve was fitted with two processes in operation, with $s_1 = 1/2$ for the first. It was found that the following parameters resulted in the best overall fit: f = 0.17, $\eta_{i1} = 2$, $s_2 = 1.55$ and $\eta_{i2} = 2.2$. Also for this sample, a nearly perfect match between experiment and theory is obtained (see Fig. 3). It should be noted that, only in the initial stages of the precipitation, does reaction process 1 contribute significantly to the overall heat flow. As a result of this, while f and S_1 can be determined with reasonable accuracy, variation of η_{i1} has nearly no influence on the quality of the fit. Because the value of s_2 is close to $1\frac{1}{2}$, process 2 corresponds to the growth of pre-existing nuclei.

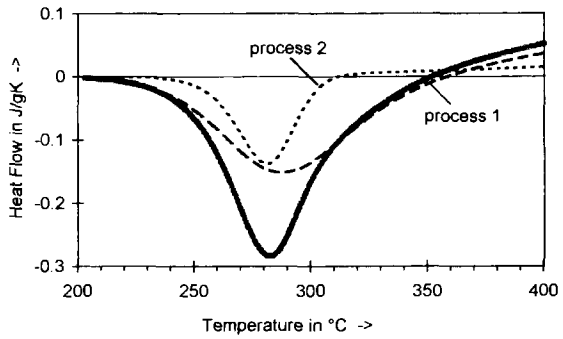

Fig. 3. DSC curve ($\beta = 20$°C/min) of Al–6 Si which was cooled at −200°C/min after solution treatment at 550°C (thick, grey line). The fit (thinner, black line) is obtained with the model presented in Section 3. Also indicated are the contributions of the two processes (dotted lines).

As a further example, we present the results for Al–6at% Si aged for 4 years after quenching in iced water. It is expected that, after this long period of natural ageing, a high density of nuclei should be present in the alloy. A high density of nuclei close to the coarse Si particles may cause precipitation on the coarse Si particles to be negligible. Using the method outlined in point (ii), it was verified that the process with lowest s value is indeed $s_1 = 1\frac{1}{2}$. Hence, precipitation should be dominated by growth on pre-existing nuclei ($s_1 = 1\frac{1}{2}$), while nucleation and growth ($s_2 = 2\frac{1}{2}$) may also occur in the later stages. Fig. 4 shows that

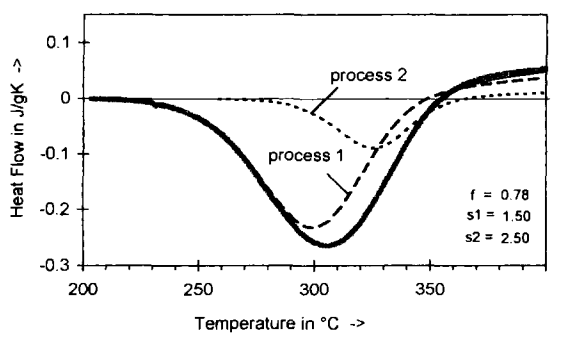

Fig. 4. DSC curve ($\beta = 20$°C/min) of Al–6 Si which was naturally aged for four years after solution treatment at 550°C (thick, grey line). The fit (thinner, black line) is obtained with the model presented in Section 3. Also indicated are the contributions of the two processes (dotted lines).

Table 1
Parameters obtained from the fits presented in Figs. 1–4

Alloy	Cooling/Ageing	f	Process 1			Process 2		
			s	η_i	Interpretation	s	η_i	Interpretation
Al–1 Si	−22 K/min	1	1.65	0.63	Growth nuclei [a]	—	—	—
Al–1 Si	IWQ+NA	0.74	1.5	0.63	Growth nuclei	2.66	2.2	Nucleation and growth [c]
Al–6 Si	−200 K/min	0.17	0.5	2	Growth particle [b]	1.55	2.2	Growth nuclei
Al–6 Si	IWQ+NA	0.78	1.5	2.2	Growth nuclei	2.5	1.4	Nucleation and growth

[a] Diffusion controlled growth of pre-existing nuclei of negligible initial size.
[b] Diffusion controlled growth of coarse particles.
[c] Nucleation and diffusion controlled growth.

a perfect match with the experimental curve can indeed be obtained with these two processes and f = 0.78.

The parameters obtained from the fits presented in Figs. 1–4 are gathered in Table 1. From this table, it is noted that values of η_i obtained from the fits (0.63 to 2.2) are in the range of the value expected for the case of impingement according to the AR equation ($\eta_i = 1$), but incompatible with impingement according to JMAK kinetics ($\eta_i = \infty$). This finding is in line with those made for a range of isothermal precipitation reactions [8], which generally also correspond much better to the AR equation (Eq. (2)) than to the JMAK equation (Eq. (1)).

5. Conclusions

A quantitative model is derived for the progress of a nucleation and growth controlled reaction during heating at a constant rate. The variation of the equilibrium state with temperature has been taken into account. Parameters of the model for a single process reaction are: s, which is akin to the Avrami parameter for isothermal analysis; E_{eff}, the effective activation energy; η_i, the impingement parameter; and a pre-exponential constant.

The model is applied to DSC data on precipitation in Al–Si alloys. An excellent agreement between data and model is found. The parameter s can be interpreted in terms of the processes occurring, namely growth of small pre-existing nuclei, growth of coarse particles and nucleation and growth. Application of the model allows the identification of the contributions of the different processes to the overall transformation.

Acknowledgements

This work is financed in part by the EC Human Capital and Mobility project. Mr. C. Zahra is thanked for performing DSC experiments.

References

[1] W.A. Johnson and K.E. Mehl, Trans. Am. Inst. Min. Met. Engrs., 195 (1939) 416.
[2] M. Avrami, J. Chem. Phys., 7 (1939) 1103.
[3] M. Avrami, J. Chem. Phys., 8 (1940) 212.
[4] M. Avrami, J. Chem. Phys., 9 (1941) 177.
[5] A.N. Kolmogorov, Izv. Akad. Nauk SSSR, Ser. Mater., 1 (1937) 355.
[6] J.W. Christian, The Theory of Transformations in Metals and Alloys, 2nd edn., Part 1, Pergamon Press, Oxford, UK (1975).
[7] F.L. Cumbrera and F. Sanchez-Bajo, Thermochim. Acta, 266 (1995) 315.
[8] M.J. Starink, submitted to J. Mater. Sci.
[9] M.J. Starink, J. Mater. Sci. Lett., 15 (1996) 1749.
[10] M.J. Starink and P. van Mourik, in: T. Khan and G. Effenberg (Eds.), Proc. of the Internat. Conf. on Advanced Al and Mg Alloys, Amsterdam, 20–22 June, 1990, ASM (1990) p. 695.
[11] C.Y. Zahra and A.-M. Zahra, Thermochim. Acta, 276 (1996) 161.
[12] M.J. Starink and A.-M. Zahra, submitted to Acta Mater.
[13] D.E. Coates, Metall. Trans., 3 (1972) 1203.
[14] E. Woldt, J. Phys. Chem. Solids, 53 (1992) 521.
[15] P. Krüger, J. Phys. Chem. Solids, 54 (1993) 1549.
[16] T.J.W. de Bruijn, W.A. de Jong and P.J. van den Berg, Thermochim. Acta, 45 (1981) 315.
[17] Eon-Sik Lee and Young G. Kim, Acta Metall. Mater., 38 (1990) 1669.
[18] E.J. Mittemeijer, J. Mater. Sci., 27 (1992) 3977.
[19] T. Ozawa, Thermochim. Acta, 203 (1992) 159.

[20] J.W. Graydon, S.J. Thorpe and D.W. Kirk, Acta Metall. Mater., 42 (1994) 3163.
[21] M.J. Starink, Thermochim. Acta, 288 (1996) 97.
[22] M. van Rooyen and E.J. Mittemeijer, Metall. Trans., 20A (1989) 1207.
[23] J.M. Criado and A. Ortega, J. Thermal Anal., 29 (1984) 1225.
[24] J.M. Criado and A. Ortega, Acta Metall., 35 (1987) 1715.
[25] H. El Sayed and I. Kovács, Phys. Stat. Sol. A, 24 (1994) 123.
[26] E. Ozawa and H. Kimura, Mater. Sci. Eng., 8 (1971) 327.
[27] E. Hornbogen, A.K. Mukhopadhyay and E.A. Starke, J. Mater. Sci., 28 (1993) 3670.
[28] M.J. Starink and A.-M. Zahra, in preparation.